Carbon Monoxide Oxidation on Metal-Supported Monolayer Oxide Films: Establishing Which Interface is Active

Ke Zhang[+], Linfei Li[+], Shamil Shaikhutdinov, and Hans-Joachim Freund*

Abstract: *Ultrathin (monolayer) films of transition metal oxides grown on metal substrates have recently received considerable attention as promising catalytic materials, in particular for low-temperature CO oxidation. The reaction rate on such systems often increases when the film only partially covers the support, and the effect is commonly attributed to the formation of active sites at the metal/oxide boundary. By studying the structure and reactivity of FeO(111) films on Pt(111), it is shown that, independent of the film coverage, CO oxidation takes place at the interface between reduced and oxidized phases in the oxide film formed under reaction conditions. The promotional role of a metal support is to ease formation of the reduced phase by reaction between CO adsorbed on metal and oxygen at the oxide island edge.*

Ultrathin films of transition-metal oxides (TMO) supported on metal substrates show unique properties owing to reduced dimensionality and strong interaction with the underlying support.[1] Among these systems, a monolayer FeO(111) film grown on Pt(111) is one of the most explored.[2] The interest in the films was reinforced after they showed considerable activity in CO oxidation at low temperatures.[3] Experimental studies and density functional theory (DFT) calculations[4] showed that a FeO(111) film transforms into an O-rich film with a close to FeO_2 stoichiometry and considered, for simplicity, as an O-Fe-O tri-layer. In fact, the O-rich films have a more complex structure, where FeO_2 tri-layer domains are embedded into the FeO film following the moiré pattern present in FeO(111)/Pt(111)[5] (Figure 1). The reaction mechanism was rationalized in terms of direct CO reaction with a weakly bonded oxygen atom in the topmost layer thus forming CO_2 that desorbs and leaves oxygen vacancy behind, which is then replenished by reaction with molecular O_2 in the gas phase.

The situation becomes more complex at sub-monolayer (sub-ML) film coverages as the surface additionally exposes oxide/metal interfacial cites, which are commonly considered to be active. Bao and co-workers[6] addressed reactivity of FeO(111) islands on Pt(111) by scanning tunneling microscopy (STM) and ultraviolet photoelectron spectroscopy (UPS) under ultrahigh vacuum (UHV) conditions. Following the reaction by O_2 exposure to the CO pre-saturated surface and measuring CO consumption rate with UPS, the authors found a linear relationship between the activity and the island perimeter. This finding allowed the authors to conclude that the reaction takes place at the FeO(111)/Pt(111) boundary. The mechanism was studied by DFT, first for FeO(111)[6] and then for other TMO(111) islands on Pt(111).[7] It has been proposed that O_2 dissociates at coordinatively unsaturated Fe sites present at the island edges, thus resulting in O atoms bound both to Fe and Pt, which react with CO adsorbed on Pt to form CO_2. A recent STM study showed that the Fe-terminated edges may, indeed, host the catalytically active sites.[8]

Although this mechanism may be operative under UHV-based conditions, it hardly holds true at the realistic pressures, which force the formation of the FeO_{2-x} phase. Indeed, the transformation of a dense FeO film into FeO_{2-x} sets in at O_2 pressures as low as 10^{-2} mbar at 300 K[4] and even in 10^{-6} mbar O_2 at about 600 K for FeO islands.[9]

Pan et al.[10] studied CO oxidation on the FeO(111)/Pt(111) films at near atmospheric pressures as a function of the film coverage. The activity vs. coverage plot showed a maximum at about 0.4 ML, indicating that the oxide/metal boundary is more active than the film surface itself. Furthermore, temperature-programmed reaction experiments only showed CO_2 production on oxidized FeO_{2-x} films, with a maximum reached at nearly the same coverage. All these results provided strong evidence that it is the FeO_{2-x}/Pt interface that catalyzes the reaction under realistic conditions. Accordingly, the enhanced reactivity was attributed to the reaction between CO adsorbed on Pt and oxygen species at the FeO_2 edges.

Even though certain progress has recently been reached towards understanding the reactivity of the FeO(111)/Pt(111) systems (see also recent studies[11]), the reaction mechanism remains poorly understood. Basically, all proposed models considered solely the boundary between the oxide (either FeO or FeO_2) and the metal surface. Herein, we provide experimental results showing that the CO oxidation reaction takes place not at oxide/metal interface, but at sites provided by the boundary between reduced and oxidized FeO_x phases in the film, the formation of which is promoted by the metal support at the initial stages of the reaction.

Figure 1a displays a typical STM image of a sub-ML oxidized FeO_{2-x} film, showing both individual islands and extended patches decorating terrace edges of the Pt(111)

[*] Dr. K. Zhang,[+] Dr. L. Li,[+] Dr. S. Shaikhutdinov, Prof. Dr. H.-J. Freund
Fritz-Haber-Institute, Max Planck Society
Faradayweg 4–6, 14195 Berlin (Germany)
E-mail: shaikhutdinov@fhi-berlin.mpg.de
Dr. K. Zhang[+]
Present address: Institute of Physics
Ecole Polytechnique Federale de Lausanne (EPFL)
1015 Lausanne (Switzerland)

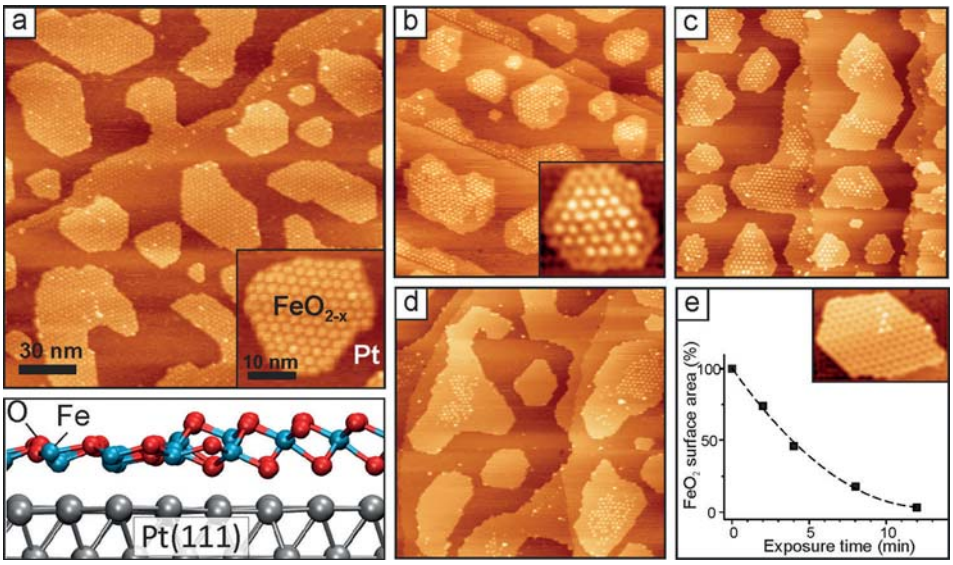

Figure 1. a) Typical morphology of oxidized FeO_{2-x} films on Pt(111) at sub-monolayer coverages. The cross-view of a FeO_{2-x}/Pt(111) film is shown below. b)–d) STM images of 0.5 ML FeO_{2-x}/Pt(111) film exposed to 10^{-6} mbar CO at 450 K for 2 min (b), additional 2 min (that is, 4 min in total) (c), and 8 min in total (d); Image size is 150 nm × 150 nm; tunneling bias and current are −3 V and 0.1 nA, respectively. e) The FeO_{2-x} surface area normalized to the area in the as-prepared sample as a function of the accumulative exposure time.

surface. A superstructure imaged as periodic protrusions of about 2.5 nm in size uniformly covers the oxide surface. The protruding spots reflect areas with a FeO_2 tri-layer structure within the moiré pattern[5] (see the model in Figure 1). Although we could not achieve high resolution to address the atomic structure of the island edges, analysis of numerous STM images[12] suggest that the island edges are rarely represented by partial protrusions (see inset in Figure 1a), indicating that an interface formed by a FeO_2 tri-layer domain to the Pt surface is a minority species. Recent STM studies[5b,13] also found a rich variety of edge structures that may exist depending on the preparation and exposure conditions.

We first studied the interaction of FeO_{2-x} islands with pure CO by exposing it to 10^{-6} mbar at 450 K for 2 min several times. Room temperature STM images, after each treatment (Figure 1b–d), clearly show that CO induced reduction starts at the island edge and propagates into the interior region, leaving a FeO(111)-like structure behind (insets in Figure 1b,e). Apparently, the reaction front velocity depends on edge orientation and size. Figure 1e depicts global kinetics of the FeO_{2-x}→FeO reduction by measuring the FeO_{2-x} surface area normalized to the total islands area. The best fit revealed areas decaying as $1-0.15t+0.006t^2$ (R factor 0.995). Such a decay is typical for etching of two-dimensional islands involving bond-breaking at the edge sites following a first-order kinetics.[14] In our case, the rate-limited step is most likely the CO reaction with an O atom to form CO_2, which desorbs into the gas phase. Indeed, the reaction considerably slows down by lowering the temperature (Supporting Information, Figure S1).

Furthermore, the STM images (Figure 2) show that the protrusions disappear starting from the side that is closer to the island edge. The interior region remains intact, indicating that no reaction occurs on the oxidized FeO_{2-x} surface. The progressive reduction only takes place at the interface between the compact FeO_{2-x} domain and the reduced surface formed by the reaction with CO.

To rationalize this behavior, we invoke DFT calculations[10] for periodic structures, which found the lowest O vacancy formation energy ($E_{vac}=1.31$ eV) for the oxygen atoms at the intrinsic FeO_2/FeO interface within the FeO_{2-x} structure. The respective energies for oxygen atoms at the FeO_2/Pt edge are 1.58 and 1.53 eV, that is, considerably lower than for surface oxygen in the FeO_2 tri-layer

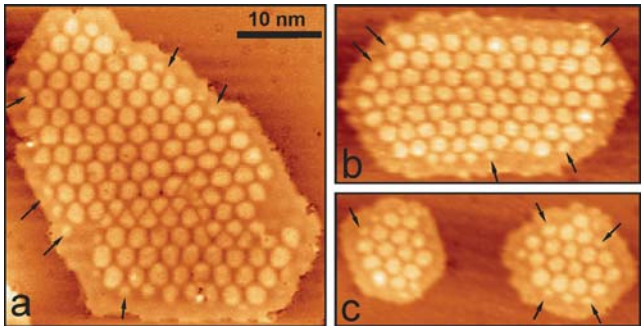

Figure 2. STM images of the FeO_{2-x} islands after exposure to 10^{-6} mbar CO at 400 K for 4 min. Tunneling conditions: bias −3 V, current 0.05 nA. The arrows highlight non-uniform disappearance of the Moiré spots close to the island edge.

(1.67 eV), and all these are much more weakly bound than the O atoms at the FeO/Pt edge (2.15 eV). The proposed scenario is shown in Figure 3. For simplicity, we considered the exposed FeO_2/metal interface. First, CO adsorbed on Pt reacts with the O atom at the island edge. The Fe atoms around the O vacancy relax and bind to Pt locally forming a FeO structure. However, further CO reaction with this site is hardly possible (under the assumptions made) as it requires about 2.15 eV to extract oxygen from FeO/Pt. Therefore, the reaction pathway involving CO on Pt(111) is terminated. However, a new interface is created, which is similar to the intrinsic FeO/FeO_2 interface. Extraction of oxygen at this interface only costs 1.31 eV,[10] thus rendering the reaction with CO feasible.

CO may either react directly with the O atom via an Eley–Rideal type mechanism or first adsorb on a neighboring low-

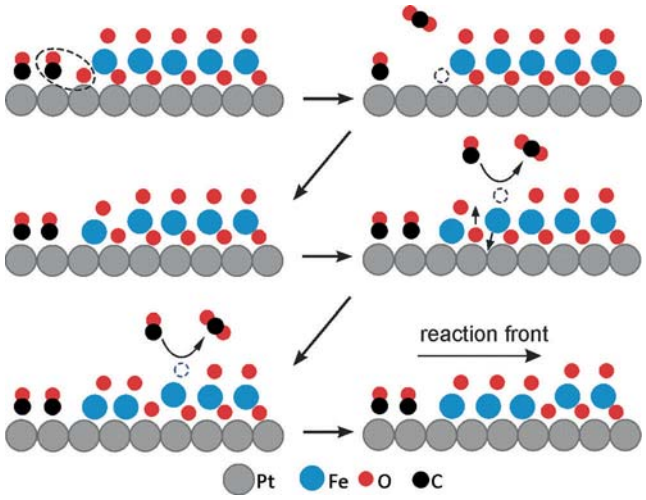

Figure 3. Scenario for CO reaction with FeO_{2-x}/Pt(111) islands. CO adsorbed on Pt reacts with the O atom at the island edge to form CO_2. The atoms surrounding the O vacancy relax and locally form a FeO bilayer structure. Further reaction occurs at the interface between the original oxidized FeO_2 and the reduced FeO-like phases, providing the most weakly bonded oxygen (see text).

coordinated Fe atom and then react via a Langmuir–Hinshelwood type mechanism. The process further repeats itself, and the interface spatially shifts towards the interior region. In principle, such a scenario can be adopted for other possible FeO_x/Pt structures at the island edge in the oxidized films. Furthermore, once triggered the reaction may also propagate along the island edge via the same mechanism. Note that even though the surface left behind the reaction front showed STM fingerprints of FeO(111), its atomic structure and hence interface to the FeO_{2-x} domains may not be exactly the same as discussed in the model. However, we took the model as a guideline.

In the next step, we studied morphological changes induced by mixtures of CO and O_2. After exposure to a stoichiometric $CO/O_2 = 2{:}1$ mixture at 450 K, STM images showed the same morphology as in pure CO (compare Figure 4b,c). Subsequent 6 min exposure to the O-rich mixture ($CO/O_2 = 1{:}5$) caused no further changes in the film (compare Figure 4c,d), whereas the film would be fully reduced in pure CO (Figure 1). Obviously, oxygen in excess suppresses oxide reduction. On the other hand, the front line does not return back toward the island edges either. Moreover, STM images of the samples directly exposed to the O-rich mixtures ($CO/O_2 = 1{:}5$ and 1:9, see Figure 4e,f) show that even excess of oxygen in the mixture cannot prevent edges from reduction. Although the reaction does not propagate far from the island edge, it is clear that the oxidized FeO_{2-x}/Pt interface does not survive under reaction conditions.

To link the observed structure and reactivity, we carried out reaction tests in another UHV chamber using a quadrupole mass-spectrometer (QMS) placed close (ca. 1 mm) to the film surface. Figure 5 (red curve) depicts the CO_2 signal recorded on the 0.5 ML FeO_{2-x}/Pt(111) sample in an O-rich mixture consisting of 1×10^{-6} mbar of CO and 5×10^{-6} mbar of O_2. After the crystal was heated up to the reaction temperature (450 K), sustained CO_2 production is observed, suggesting that the prepared surface is catalytically active. The reaction rate stays fairly constant, at least within the first 10 min. In the next experiment, we stopped the oxygen flow after 2 min of the reaction at 450 K (Figure 5, black curve). As expected, the CO_2 production drops to zero and recovers after re-introducing O_2. However, the CO_2 signal does not reach the original level. This is more clearly seen by switching oxygen off and on. The steady-state activity almost linearly decreases with increasing the number of pulses. Bearing in mind that FeO_{2-x} islands in pure CO ambient (that is, when O_2 is off) exhibit progressive reduction propagating from the edge (Figure 2), which cannot be recovered even in oxygen-rich ambient (Figure 4c,d), the observed rate attenuation can

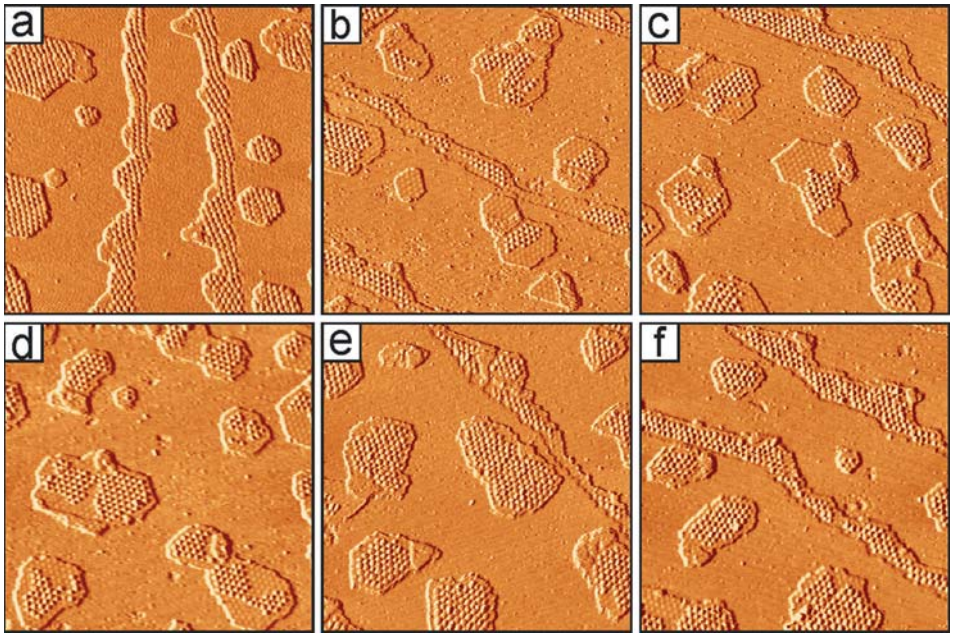

Figure 4. a)–c) STM images (presented in differentiated contrast) of the oxidized FeO_{2-x} sample before (a) and after exposure to 10^{-6} mbar CO (b). The same sample was re-oxidized and exposed to the mixture of 5×10^{-7}mabr O_2 and 10^{-6} mbar CO (c). d) The same sample as in (c) after additional exposure to the mixture of 5×10^{-6} mbar O_2 and 10^{-6} mbar CO. e) Oxidized FeO_{2-x} sample after exposure to the mixture of 5×10^{-6} mbar O_2 and 10^{-6} mbar CO. f) Oxidized FeO_{2-x} sample after exposure to the mixture of 9×10^{-6} mbar O_2 and 10^{-6} mbar CO. All gas exposures were performed at 450 K for 6 min. Image size is 150 nm × 150 nm, the tunneling conditions are a) −2.3 V, 1.9 nA; b)–d) −2.1 V, 1.9 nA; e),f) −3.0 V, 1.9 nA.

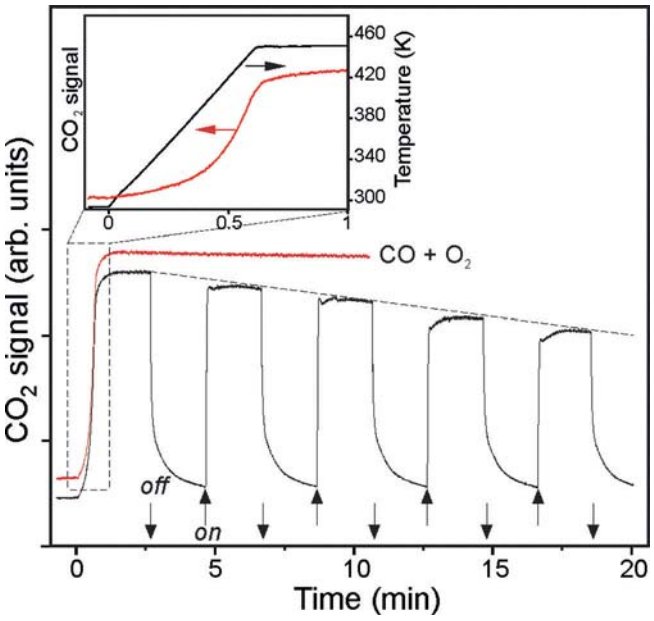

Figure 5. CO_2 (44 amu) signal measured by QMS in front of the submonolayer FeO_{2-x} film. The reaction ($CO/O_2 = 1:5$) mixture consisting of 10^{-6} mbar of CO and 5×10^{-6} mbar of O_2. At time zero, the sample was heated up to the reaction temperature 450 K with a rate 2 K s^{-1}. The red curve shows CO_2 production under steady state conditions. The black curve shows CO_2 kinetics upon switching O_2 flow in the mixture off and on, as indicated by the arrows, while keeping the CO pressure constant.

readily be explained by decreasing the total perimeter length of the boundary between the oxidized FeO_{2-x} and reduced FeO-like phases. Therefore, the results provide compelling evidence that this interface provides the most active sites.

It is important to note that a similar picture has previously been observed by STM on continuous FeO_{2-x} films on Pt(111) treated in the mbar pressure range, where compact domains of FeO_{2-x} were surrounded by areas formed upon reduction with CO.[15] It has been proposed that the reduction process starts on some defects. In the case of partially covered films, the transformation is definitely triggered at the island edges via reaction with CO adsorbed on Pt. Certain similarities between the results on dense FeO films at high pressures[15] and those obtained in this study for FeO islands at low pressures, suggest that the reaction in both cases occurs at the interface between the reduced (red) and the oxidized (ox) phases of the film formed under reaction conditions, that is, on the $oxide_{red}/oxide_{ox}$ interface, irrespectively of the film coverage. The observed coverage effect[10] may be linked to the easy formation of the reduced phase via reaction between CO adsorbed on Pt and oxygen at the oxide island edge in partially covered films. Therefore, Pt may be considered as a promoter for the formation of the active interface rather than directly participating in the catalytic reaction.

In summary, by studying structure and reactivity of submonolayer FeO(111)/Pt(111) films we provide strong evidence that the CO oxidation reaction primarily takes place at the oxide/oxide interface in the film, the formation of which is promoted by the Pt support, and not directly at the oxide/Pt interface as considered previously. In addition, the results show that certain precautions must be taken into account while applying the concept of inverted, that is, oxide-on-metal model catalysts to mimic reactions occurring on conventional metal catalysts supported on transition metal oxides. It becomes evident that the two-dimensional character of the iron oxide film is important for the structure–reactivity relationships observed. Indeed, iron oxide nanoparticles formed on Pt(111) as a result of FeO film dewetting[3] were found to be inactive, although expose a metal/oxide interface. This may hold true for other ultrathin film systems as well. Finally, our results may shed light on the origin of reactivity of unsupported iron oxide catalysts, the activity of which is usually associated with low-coordinated sites that may readily be formed at the above-discussed oxide/oxide interfaces.

Experimental Section

The experiments were performed in an UHV chamber equipped with LEED, AES, and STM. FeO(111) films were prepared using the method reported in Ref. [9] by evaporating Fe onto the Pt surfaces in 1.3×10^{-7} mbar O_2 at 300 K followed by annealing in 1×10^{-6} mbar O_2 at 700 K for 5 min. As-prepared FeO(111) samples were oxidized in 5×10^{-6} mbar O_2 at 570 K to transform into the FeO_{2-x} phase. STM images were obtained using electrochemically etched W-tips. Reactivity measurements were performed in another UHV chamber equipped with QMS. The films were prepared in the same manner as described above, and the coverage was determined by CO titration of Pt(111) using TPD spectra of 2 L CO adsorbed at 300 K.[10]

Acknowledgements

This work was supported by Fonds der Chemischen Industrie. We thank the German Research Foundation for support through the cluster of excellence UNICAT administered by the Technical University berlin. We also thank Livia Giordano for providing us the DFT-optimized FeO_{2-x} structure shown in Figure 1.

Conflict of interest

The authors declare no conflict of interest.

Keywords: CO oxidation · inverse catalysts · iron oxide · metal/oxide interface · ultrathin oxide films

How to cite: *Angew. Chem. Int. Ed.* **2018**, *57*, 1261–1265
Angew. Chem. **2018**, *130*, 1275–1279

[1] a) G. Pacchioni, *Chem. Eur. J.* **2012**, *18*, 10144–10158; b) *Oxide Materials at the Two-Dimensional Limit* (Eds.: F. P. Netzer, A. Fortunelli), Springer, Cham, Switzerland, **2016**; c) H.-J. Freund, *J. Am. Chem. Soc.* **2016**, *138*, 8985–8996.

[2] a) G. H. Vurens, M. Salmeron, G. A. Somorjai, *Surf. Sci.* **1988**, *201*, 129–144; b) L. Giordano, G. Pacchioni, J. Goniakowski, N. Nilius, E. D. L. Rienks, H.-J. Freund, *Phys. Rev. B* **2007**, *76*, 075416; c) L. R. Merte, J. Knudsen, L. C. Grabow, R. T. Vang, E. Lægsgaard, M. Mavrikakis, F. Besenbacher, *Surf. Sci.* **2009**, *603*, L15–L18.

[3] Y. N. Sun, Z. H. Qin, M. Lewandowski, E. Carrasco, M. Sterrer, S. Shaikhutdinov, H. J. Freund, *J. Catal.* **2009**, *266*, 359–368.

[4] Y.-N. Sun, L. Giordano, J. Goniakowski, M. Lewandowski, Z.-H. Qin, C. Noguera, S. Shaikhutdinov, G. Pacchioni, H.-J. Freund, *Angew. Chem. Int. Ed.* **2010**, *49*, 4418 – 4421; *Angew. Chem.* **2010**, *122*, 4520 – 4523.
[5] a) L. Giordano, M. Lewandowski, I. M. N. Groot, Y. N. Sun, J. Goniakowski, C. Noguera, S. Shaikhutdinov, G. Pacchioni, H. J. Freund, *J. Phys. Chem. C* **2010**, *114*, 21504 – 21509; b) L. R. Merte, Y. Bai, H. Zeuthen, G. Peng, L. Lammich, F. Besenbacher, M. Mavrikakis, S. Wendt, *Surf. Sci.* **2016**, *652*, 261 – 268.
[6] Q. Fu, W.-X. Li, Y. Yao, H. Liu, H.-Y. Su, D. Ma, X.-K. Gu, L. Chen, Z. Wang, H. Zhang, B. Wang, X. Bao, *Science* **2010**, *328*, 1141 – 1144.
[7] D. Sun, X.-K. Gu, R. Ouyang, H.-Y. Su, Q. Fu, X. Bao, W.-X. Li, *J. Phys. Chem. C* **2012**, *116*, 7491 – 7498.
[8] W. Kudernatsch, G. Peng, H. Zeuthen, Y. Bai, L. R. Merte, L. Lammich, F. Besenbacher, M. Mavrikakis, S. Wendt, *ACS Nano* **2015**, *9*, 7804 – 7814.
[9] Q. Fu, Y. Yao, X. Guo, M. Wei, Y. Ning, H. Liu, F. Yang, Z. Liu, X. Bao, *Phys. Chem. Chem. Phys.* **2013**, *15*, 14708 – 14714.
[10] Q. Pan, X. Weng, M. Chen, L. Giordano, G. Pacchioni, C. Noguera, J. Goniakowski, S. Shaikhutdinov, H.-J. Freund, *ChemCatChem* **2015**, *7*, 2620 – 2627.
[11] a) L. R. Merte, C. J. Heard, F. Zhang, J. Choi, M. Shipilin, J. Gustafson, J. F. Weaver, H. Grönbeck, E. Lundgren, *Angew. Chem. Int. Ed.* **2016**, *55*, 9267 – 9271; *Angew. Chem.* **2016**, *128*, 9413 – 9417; b) N. Johansson, L. R. Merte, E. Grånäs, S. Wendt, J. N. Andersen, J. Schnadt, J. Knudsen, *Top. Catal.* **2016**, *59*, 506 – 515.
[12] a) H. Chen, Y. Liu, F. Yang, M. Wei, X. Zhao, Y. Ning, Q. Liu, Y. Zhang, Q. Fu, X. Bao, *J. Phys. Chem. C* **2017**, *121*, 10398 – 10405; b) Y. Liu, F. Yang, Y. Zhang, J. Xiao, L. Yu, Q. Liu, Y. Ning, Z. Zhou, H. Chen, W. Huang, P. Liu, X. Bao, *Nat. Commun.* **2017**, *8*, 14459.
[13] H. Zeuthen, W. Kudernatsch, L. R. Merte, L. K. Ono, L. Lammich, F. Besenbacher, S. Wendt, *ACS Nano* **2015**, *9*, 573 – 583.
[14] Z.-J. Wang, J. Dong, Y. Cui, G. Eres, O. Timpe, Q. Fu, F. Ding, R. Schloegl, M.-G. Willinger, *Nat. Commun.* **2016**, *7*, 13256.
[15] M. Lewandowski, I. M. N. Groot, S. Shaikhutdinov, H. J. Freund, *Catal. Today* **2012**, *181*, 52 – 55.

Manuscript received: October 24, 2017
Revised manuscript received: November 22, 2017
Accepted manuscript online: December 13, 2017
Version of record online: January 4, 2018